ELSEVIER

Atherosclerosis 186 (2006) 374–379

ATHEROSCLEROSIS

www.elsevier.com/locate/atherosclerosis

Sustained progression and loss of the gender-related difference in atherosclerosis in the very old: A pathological study of 1074 consecutive autopsy cases

Motoji Sawabe [a,*], Tomio Arai [a], Ichiro Kasahara [a], Akihiko Hamamatsu [a], Yukiyoshi Esaki [a,1], Ken-ichi Nakahara [b,2], Kazumasa Harada [b], Kouji Chida [b], Hiroshi Yamanouchi [b], Toshio Ozawa [b], Kaiyo Takubo [c], Shigeo Murayama [d], Noriko Tanaka [e]

[a] *Department of Pathology, Tokyo Metropolitan Geriatric Hospital, 35-2 Sakae-cho, Itabashi, Tokyo 173-0015, Japan*
[b] *Department of Internal Medicine, Tokyo Metropolitan Geriatric Hospital, Tokyo, Japan*
[c] *Human Tissue Research Group, Tokyo Metropolitan Institute of Gerontology, Tokyo, Japan*
[d] *Geriatric Neuroscience Research Group, Tokyo Metropolitan Institute of Gerontology, Tokyo, Japan*
[e] *Department of Clinical Bioinformatics, Graduate School of Medicine, Tokyo University, Tokyo, Japan*

Received 24 May 2005; received in revised form 9 July 2005; accepted 18 July 2005
Available online 29 August 2005

Abstract

Introduction: Epidemiological surveys show decrease or reversal of male predominance in cardiovascular mortality in the very old, but the actual condition of atherosclerosis in the very old is largely unknown. The objective of this paper is to reveal whether the atherosclerosis continues to progress, or the gender-related difference exists in the very old.
Methods: The subjects were 1074 consecutive autopsy cases of in-hospital death. The male:female ratio was 1.1:1 and the average age was 80 years. Macroscopic evaluation was performed on the degree of atherosclerosis in 10 arteries including the intracranial arteries, carotid artery, aorta, coronary artery, and femoral artery.
Results: The severity of atherosclerosis differed greatly among arteries. The age-related increase of the atherosclerotic degree was evident, even after 80 years of age. The atherosclerosis was more severe in males than in females in their 60s, but this male predominance decreased with ageing and finally disappeared in their 90s.
Conclusion: The sustained progression of atherosclerosis and loss of the gender-related difference probably account for the increase of cardiovascular mortality in very old females. They also suggest that the prevention of the atherosclerotic progression is still important in the seventh and eighth decade of life.

Keywords: Aging; Atherosclerosis; Pathology; Autopsy; Gender-difference

1. Introduction

Atherosclerosis causes a large number of complications, such as cerebrovascular disease, coronary heart disease, ischemic bowel disease, renovascular hypertension, Leriche syndrome, peripheral arterial disease, and aneurysms. Chronic disseminated intravascular coagulation and elevated inflammatory markers, such as highly sensitive C-reactive protein, are reported to be other manifestations of atherosclerosis. Atherosclerosis, however, is also a sub-

Abbreviations: CHD, coronary heart disease; CSI, coronary stenotic index; CT, computer tomography; ICAI, intracranial atherosclerotic index; JG-SNP, the Japanese SNP database for geriatric research; MRI, magnetic resonance imaging; PAI, pathological atherosclerotic index

* Corresponding author. Tel.: +81 3 3964 1141; fax: +81 3 3964 1982.
E-mail address: sawabe@tmig.or.jp (M. Sawabe).
[1] Present address: Department of Pathology, Sekishinkai Sayama Hospital, Saitama, Japan.
[2] Present address: Medical Division, Nagasaki Medical Center, Omura, Japan.

0021-9150/$ – see front matter © 2005 Elsevier Ireland Ltd. All rights reserved.
doi:10.1016/j.atherosclerosis.2005.07.023

clinical entity because it does not always result in these complications even in cases with severe atherosclerosis. It is, therefore, difficult to speculate on the severity of atherosclerosis only from the presence of these complications. The clinical assessment of atherosclerosis is a challenging subject and the pathological study by autopsy is still the most reliable assessment method of systemic atherosclerosis.

Although several pathological studies have been reported regarding the severity of atherosclerosis [1–8], very little information was available about atherosclerosis in the elderly, especially in people of more than 80 years of age. It is still unknown whether atherosclerosis continues to progress in the very old, or whether the gender-related difference exists in the elderly because decades have passed since the menopause in female subjects. Recent epidemiological surveys showed decrease or reversal of the male predominance in cardiovascular mortality in the very old both in Japan and the U.S. [9,10], but the exact cause was unspecified. To address these issues, we performed a comprehensive pathological study in more than 1000 consecutive autopsy cases. This is the first pathological report analyzing the gender-specific, age-related changes of atherosclerosis in the very elderly.

2. Subjects and methods

2.1. Subjects

The subjects were 1074 consecutive elderly autopsy cases performed at Tokyo Metropolitan Geriatric Hospital, Tokyo, Japan from 1995 to 2000. The details of the subjects including major clinical diagnosis and direct causes of death examined by autopsy are summarized in Table 1. We have been presenting our autopsy cases on an Internet-based database on the web since April 2003, which was named "The Japanese SNP database for geriatric research (JG-SNP)" located at http://www.tmgh.metro.tokyo.jp/jg-snp/english/E_top.html, as was previously reported [11]. The JG-SNP included all the subjects used in this study. The subjects did not include any medicolegal cases.

Tokyo Metropolitan Geriatric Hospital is a community-based general hospital for the aged and has all medical departments except Obstetrics and Pediatrics. Over 90% of the outpatients come from the neighboring wards or cities of Tokyo. The average day of hospitalization had decreased during the observation period from 45.6 days in 1995 to 24.3 days in 2000. The average autopsy rate in this period was 40% in whom the brain was available in 85%.

2.2. Pathological assessment of atherosclerosis

The method of the pathological assessment of atherosclerosis was recently reported [12]. Briefly, the varying degree of atherosclerosis in eight large arteries was evaluated by macroscopic examination of the luminal surface in the formalin-fixed arteries. The eight large arteries included the common carotid artery, subclavian artery, aorta, splenic artery, superior mesenteric artery, common iliac artery, external iliac artery, and left femoral artery. The atherosclerotic degree was scored according to the ratio of the occupying atheroma to the entire intimal area: from 0 (absent, less than 1/20 of the intimal areas occupied by the atheroma), 2 (minimal, 1/20–1/6), 4 (mild, 1/6–1/3), 6 (moderate, 1/3–2/3) to 8 (severe, 2/3–1). A comparison was made to the standard grading method proposed by the American Heart Association in 1968 [13]. The grading panel of AHA and corresponding scores in our scale are shown in Fig. 1.

The pathological atherosclerotic index (PAI) was defined as the average atherosclerotic degree of these eight arteries. The coronary stenotic index (CSI) was studied according to the previous report [14]. Examination of the coronary scle-

Table 1
Clinical summary of the patients

Gender	Males	Females
Number of cases	565	509
Age at death (year)		
45–59	5	7
60–69	63	41
70–79	220	144
80–89	217	203
90–104	60	114
Mean age[a]	79.2 ± 8.1 (52–102)	81.8 ± 9.5 (47–104)
Body mass index (kg/m^2)[a]	16.9 ± 3.4 (10.7–28.4)	17.2 ± 4.0 (8.4–37.9)
History of smoking	382/519 (73.6%)	98/445 (22.0%)
Clinical diagnoses (%)		
Cerebrovascular disease[b]	187 (33.1%)	157 (30.8%)
Coronary heart disease[c]	96 (17.0%)	77 (15.1%)
Aneurysm	27 (4.8%)	17 (3.3%)
Peripheral arterial disease	24 (4.2%)	17 (3.3%)
Hypertension	131 (23.2%)	134 (26.3%)
Diabetes mellitus	78 (13.8%)	63 (12.4%)
Hyperlipidemia	11 (1.9%)	6 (1.2%)
Direct causes of death (%)[d]		
Cardiovascular events	70 (15.3%)	76 (18.3%)
Cerebral infarctions or hemorrhages	14 (3.1%)	24 (5.8%)
Myocardial infarction	43 (9.4%)	37 (8.9%)
Other events[e]	13 (2.8%)	15 (3.6%)
Pneumonia	141 (30.8%)	71 (17.1%)
Malignancy	160 (34.9%)	138 (33.3%)

[a] The figures are the averages ± S.D. and ranges in parentheses.
[b] The clinical diagnosis of cerebrovascular disease was based on neurological signs and symptoms usually with radiological evidences, which includes transient ischemic attack, reversible ischemic neurological deficit, subarachnoid hemorrhage, cerebral hemorrhage, and cerebral infarction.
[c] The coronary heart disease includes angina pectoris and myocardial infarction.
[d] The direct causes of death are determined by autopsy findings of 872 cases (458 males and 414 females) among the subjects.
[e] The other cardiovascular events include aneurysmal rupture, intestinal infarction, and severe peripheral arterial disease.

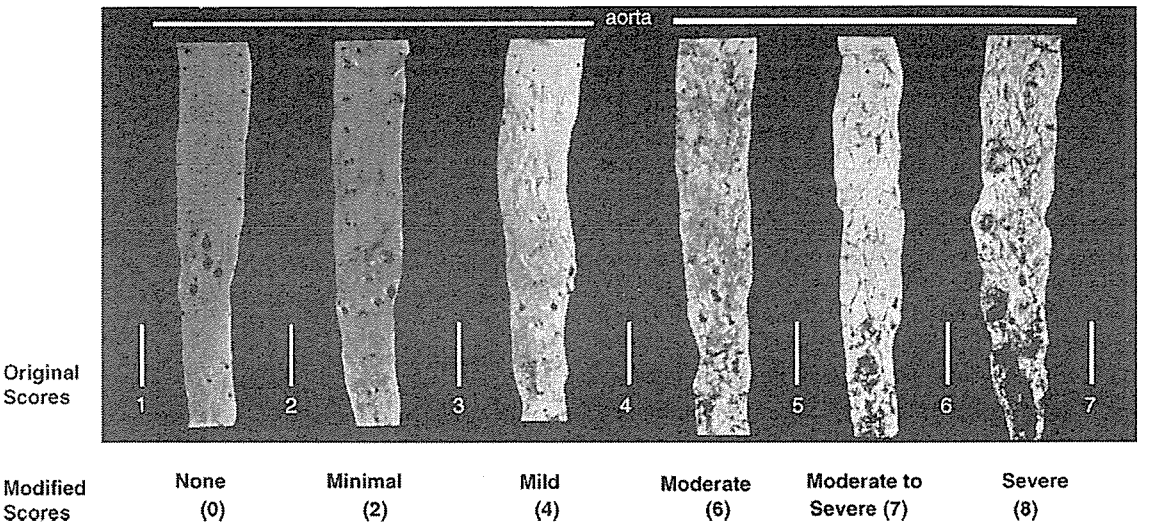

Fig. 1. Grading panel for atherosclerotic lesions, issued by the Committee on grading lesion, Council of Atherosclerosis, American Heart Association. The photographs show the aorta with different grades of atherosclerosis. Corresponding modified scores of our scale are shown beneath the original scores from 0 to 8. Reprint from the article by McGill et al. [13] with permission.

rosis was made by transverse section at 5 mm intervals. The degree of coronary stenosis was scored from 0 to 5: 0 in no sclerosis, 1 in slight stenosis, 2 in 25% stenosis, 3 in 50%, 4 in 75%, and 5 in 100% obstruction. The CSI was the sum of the stenotic scores of the three branches; left anterior descending branch, left circumflex branch, and right coronary artery. The intracranial atherosclerotic index (ICAI) was examined as previously reported [15]. The cut sections of the intracranial arteries were observed and the degree of stenosis was scored from 0 to 3: 0 in no stenosis, 0.5 in the cases only with fatty streaks, 1 in less than 50% stenosis, 2 in 50% to 90% stenosis, and 3 in 90% stenosis to occlusion. The ICAI was the sum of the stenotic scores of the left and right middle cerebral arteries and basilar artery.

2.3. Interobserver and intraobserver variations

The Bland–Altman analysis was performed for statistical analysis of interobserver and intraobserver variations, as shown in Fig. 2 [16]. The assessment was performed by two of the authors on 180 arteries derived from 15 cases. The mean difference was 0.5 (95% confidence interval; 0.3–0.7), while the upper and lower 95% limits of agreement were 3.3 (3.3–3.7) and −2.3 (−2.7 to −2.0), respectively. The standard deviation of intraobserver differences was 1.3. Considering the range from zero to eight of the atherosclerotic degree, the interobserver and intraobserver variations seemed acceptable.

2.4. Statistical analysis

A Mann–Whitney test was performed to compare the atherosclerotic degrees in the individual arteries between genders. The interobserver and intraobserver variations were assessed by the Bland and Altman plot analysis [16]. The difference between the atherosclerotic degrees assessed by the different observer against their mean was plotted to examine the interobserver variation. Repeatability was similarly

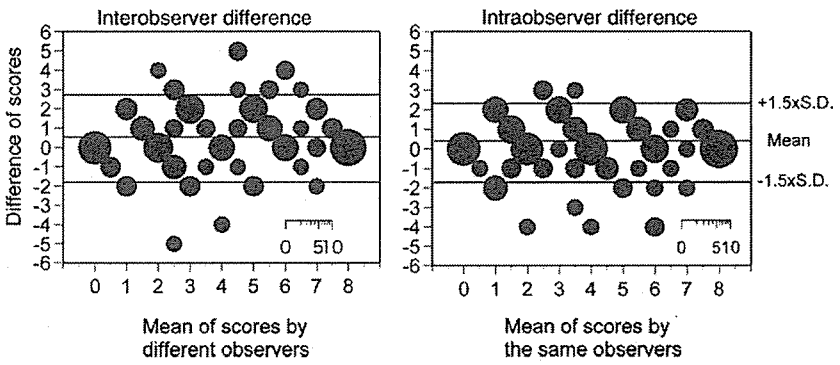

Fig. 2. Bland–Altman plot for statistical analysis of interobserver and intraobserver differences. The assessment was performed on 180 arteries derived from 15 cases. The areas of the circles represent the number of the cases.

assessed by plotting the difference between the atherosclerotic degrees assessed by the same observer against their mean. The statistical significance level was set at 0.05. The SAS system for Windows (Version 8.1) and JMP (Version 5.1) (SAS Institute Inc., NC) were used for the statistical analyses.

2.5. Ethical considerations

Written informed consent was obtained from the bereaved family of each of the patients prior to the autopsy examination. The use of autopsy materials for medical education and research is generally permitted by the Act of Postmortem Examinations of Japan.

3. Results

3.1. Distribution of the atherosclerotic degrees

Fig. 3 shows the distribution of the atherosclerotic degrees of the eight large arteries, PAI, CSI, and ICAI. The medians were high in the common iliac artery and aorta, while they were low in the splenic and superior mesenteric arteries. Variations in the degree of atherosclerosis were large in the external iliac and femoral arteries. The average (±S.D.) of the PAI, CSI, and ICAI were 3.9 (±1.5), 8.2 (±3.5), and 2.8 (±2.1), respectively. The atherosclerotic degree of the subclavian artery, PAI, and CSI followed a Normal distribution (Gaussian).

3.2. Gender-specific, age-related changes of the atherosclerotic degrees

The age-related increase in the degree of atherosclerosis was evident in both genders, as shown in Fig. 4. The atherosclerotic degree is the highest in the aorta, followed by the femoral artery, common carotid artery, and superior mesenteric artery. For subjects in their 60s and 70s, the degree of atherosclerosis is statistically higher in males than in females in most arteries, but no statistical differences are observed when subjects reach their 90s. Namely, the gender-related differences subsequently reduced with ageing and finally disappeared in their 90s. The changing rate of the age-related increase in the degree of atherosclerosis, namely the slope of the line graphs, was especially high in the femoral artery.

The average CSI was statistically higher in males than in females in their 60s and 70s, as shown in Fig. 5. The age-

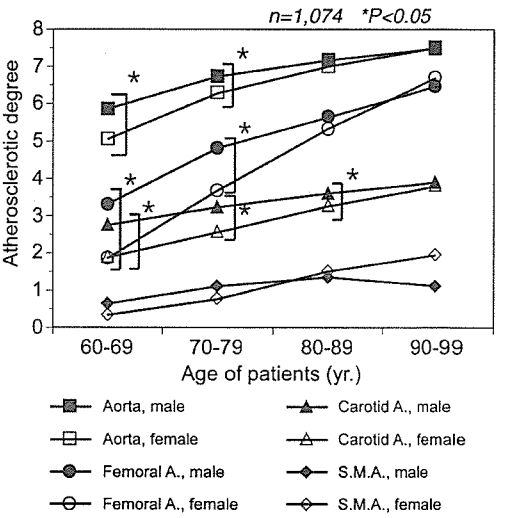

Fig. 4. Gender-specific, age-related changes of the degree of atherosclerosis in the individual arteries. S.M.A.; superior mesenteric artery. (■) Aorta, male; (□) aorta, female; (●) femoral A., male; (○) femoral A., female; (▲) carotid A., male; (△) carotid A., female; (◆) S.M.A., male; (◇) S.M.A., female.

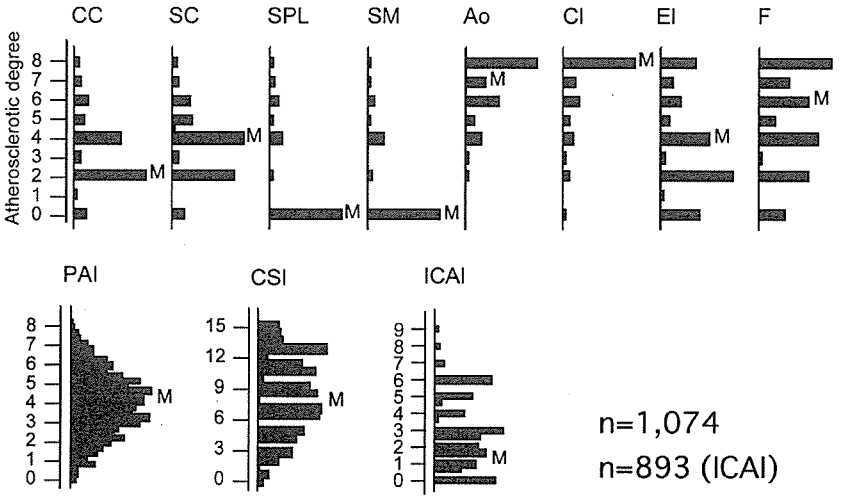

Fig. 3. Severity of atherosclerosis in the individual arteries. Ao, aorta; CC, common carotid artery; CI, common iliac artery; CSI, coronary stenotic index; EI, external iliac artery; F, femoral artery; ICAI, intracranial atherosclerotic index; M, median of the atherosclerotic degrees or indices; PAI, pathological atherosclerotic index; SC, subclavian artery; SM, superior mesenteric artery; SPL, splenic artery.

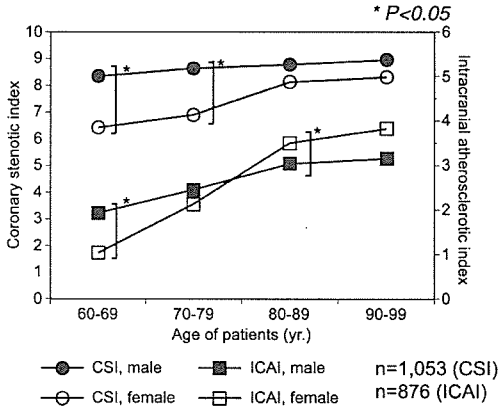

Fig. 5. Gender-specific, age-related changes of the coronary stenotic index (CSI) and intracranial atherosclerotic index (ICAI). (●) CSI, male; (○) CSI, female; (■) ICAI, male; (□) ICAI, female.

related increase of ICAI was larger in females than in males. In their 80s, the ICAI was statistically even higher in females than in males.

4. Discussion

4.1. Distribution of the atherosclerotic degrees

The present study revealed the severity of atherosclerosis differed by the arterial segments. The aorta and arteries of the lower extremities were severely affected, while the abdominal arteries, such as the splenic and superior mesenteric arteries, were mildly affected. These results were consistent with previous reports stating the abdominal aorta and common iliac arteries were the most severe sites of atherosclerotic involvement [1,2,4].

4.2. Gender-specific, age-related changes of the atherosclerotic degrees

Atherosclerosis continued to progress in the elderly in most arteries except for the coronary artery in males. Males in their 60s were more severely affected by atherosclerosis than age-matched females, but this gender-related difference reduced with ageing and finally disappeared in subjects in their 90s. In the case of the intracranial arteries and superior mesenteric artery, atherosclerosis was even more severe in females than in males in their 80s or 90s. The loss of the gender difference of atherosclerosis in the very old seems to influence the mortality. In Japan, the mortalities from heart diseases and cerebrovascular diseases are higher in males than in females in all age groups [9] and the gender differences in mortality increase with ageing, peak at 85–89 years and decrease thereafter in both diseases. A similar trend is present in the death rates from heart diseases in the U.S. [10]. The death rates from cerebrovascular diseases in the U.S. are almost even in each age group except for that of 85 years and over, in whom female predominance is evident. The loss of the gender-related difference in atherosclerosis in the very old seems responsible for the decrease or reversal of male predominance in cardiovascular mortality in the very old. Our results also suggest that the prevention of the atherosclerotic progression is still necessary in the very old, especially in females.

4.3. Limitations of the study

The subjects of this study were autopsy cases of the patients in a geriatric hospital. Therefore, we need to evaluate whether the subjects represent a hospitalized population or the demographics in Japan. The general prevalence of the major underlying diseases over 70 years of age was as follows: 29.5% in males versus 28.5% in females in hypertension (systolic blood pressure $\geq$160 Torr or diastolic blood pressure $\geq$95 Torr), 11.6% versus 21.3% in diabetes mellitus (under diabetic control or HbA1c $\geq$ 6.1%), and 15.8% versus 38.5% in hyperlipidemia (total cholesterol $\geq$ 220 mg/dl) [17]. The figures were similar to those of our results except for hyperlipidemia. Considering the low average BMI of the subjects (17 kg/m^2), the undernourished conditions seemed to contribute to the low incidence of hyperlipidemia. The death rates per 100,000 over 75 years of age in Japan were as follows: 1027.6 in males versus 860.1 in females in the cerebrovascular diseases, 537.9 versus 398.5 in ischemic heart disease, 1017.6 versus 571.4 in pneumonia, and 2085.7 versus 980.0 in malignancy [9]. The frequency of cerebrovascular diseases seems higher than our autopsy data. Since the subjects comprised entirely of the Japanese race except for one Korean and the national health insurance covers the whole population in Japan, the selection bias from the racial and socioeconomic differences of the subjects seems minimal. Altogether our subjects may represent the general population in Japan.

4.4. Perspectives

Atherosclerosis is a multifactorial disease and 30–66% of the variation of the atherosclerosis could be explained by the genetic factors [18–20]. In this context, the roles of the genetic polymorphism have been extensively studied to identify the most responsible genes for atherosclerosis. Since the postmortem pathological evaluation of the atherosclerosis is more accurate than other clinical methods, a few autopsy studies have been conducted for the genetic studies, including Helsinki Sudden Death Study [21,22] and Pathological Determinants of Atherosclerosis in Youth Study [23,24]. Both studies examined the aortic and coronary atherosclerosis in large numbers of forensic autopsy cases of sudden death and analyzed the correlations between the genetic polymorphism and the pathologically verified atherosclerosis. We also have been engaged in the researches of the genetic polymorphism of atherosclerosis, based on the autopsy cases used in this study. In the course of our study, we have obtained several

interesting results, including those appeared in this paper. We hope to identify relevant genetic polymorphic sites of the candidate genes for atherosclerosis.

Acknowledgements

The authors appreciate the assistance extended for the database-input by Ms. Makiko Naka and Ms. Mari Saito from the Department of Biostatistics, Graduate School of Medicine, University of Tokyo, and Ms. Sachiko Kobayashi. We are also grateful for the help to all the staff members of our Department of Pathology, especially to autopsy assistants, Mr. Ken-ichi Koizumi and Mr. Masao Sekii. This work was financially supported by grants from Comprehensive Research on Aging and Health (16090101), Ministry of Health, Labour and Welfare, Japan, distributed to Dr. Takuji Shirasawa (Representative), Tokyo Metropolitan Institute of Gerontology, and by the grant-in-aid from Mitsui Sumitomo Insurance Welfare Foundation.

References

[1] Roberts JC, Moses C, Wilkins RH. Autopsy studies in atherosclerosis. I. Distribution and severity of atherosclerosis in patients dying without morphologic evidence of atherosclerotic catastrophe. Circulation 1959;20:511–9.
[2] Roberts JC, Wilkins RH, Moses C. Autopsy studies in atherosclerosis. II. Distribution and severity of atherosclerosis in patients dying with morphologic evidence of atherosclerotic catastrophe. Circulation 1959;20:520–6.
[3] Strong JP, McGill Jr HC. The natural history of aortic atherosclerosis: relationship to race, sex, and coronary lesions in New Orleans. Exp Mol Pathol 1963;52(1):15–27. Suppl.
[4] Solberg LA, McGarry PA, Moossy J, Strong JP, Tejada C, Löken AC. Severity of atherosclerosis in cerebral arteries, coronary arteries, and aortas. Ann NY Acad Sci 1968;149:956–73.
[5] Bjurulf P. Atherosclerosis in different parts of the arterial system. Am Heart J 1964;68:41–50.
[6] Reiner L, Jimenez FA, Rodriguez FL. Atherosclerosis in the mesenteric circulation. Observations and correlations with aortic and coronary atherosclerosis. Am Heart J 1963;66:200–9.
[7] Larsen E, Johansen AA, Andersen D. Gastric arteriosclerosis in elderly people. Scand J Gastroenterol 1969;4(4):387–9.
[8] Järvinen O, Laurikka J, Sisto T, Salenius J-P, Tarkka MR. Atherosclerosis of the visceral arteries. Vasa 1995;24:9–14.
[9] Statistics and Information Department, Ministry of Health, Labour and Welfare, Japan. Vital Statistics, Abridged Life Tables for Japan; 2003. Available at http://www.mhlw.go.jp/english/database/db-hw/index.html (in English) or http://www.mhlw.go.jp/toukei/saikin/hw/jinkou/geppo/nengai03/index.html (in Japanese). Accessed on July 10, 2005.
[10] U.S. Census Bureau. Statistical Abstract of the United States 2004–2005, Section 2. Vital Statistics, Table No. 107 and 108; 2005. Available at: http://www.census.gov/prod/www/statistical-abstract-03.html. Accessed on July 10, 2005.
[11] Sawabe M, Arai T, Kasahara I, et al. Development of a geriatric autopsy database and internet-based database of Japanese single nucleotide polymorphisms for geriatric research (JG-SNP). Mech Ageing Dev 2004;125:547–52.
[12] Sawabe M, Takahashi R, Matsushita S, et al. Aortic pulse wave velocity and the degree of atherosclerosis in the elderly: a pathological study based on 304 autopsy cases. Atherosclerosis 2005;179:345–51.
[13] McGill Jr HC, Brown BW, Gore I, et al. Report of Committee on grading lesions, council on arteriosclerosis, American Heart Association. Grading human atherosclerotic lesions using a panel of photographs. Circulation 1968;37:455–9.
[14] Chida K, Ohkawa S, Watanabe C, Shimada H, Ohtsubo K, Sugiura M. A morphological study of the normally aging heart. Cardiovasc Pathol 1994;3:1–7.
[15] Koyama S, Saito Y, Yamanouchi H, et al. Marked decrease of intracranial atherosclerosis in contrast with unchanged coronary artery stenosis in Japan. Nippon Ronen Igakkai Zasshi (Jpn J Geriat) 2003;40:267–73 (in Japanese with English abstract).
[16] Bland JM, Altman DG. Statistical methods for assessing agreement between two methods of clinical measurement. Lancet 1986;1:307–10.
[17] Ministry of Health, Labour and Welfare, Japan. The National Nutrition Survey in Japan. Tokyo: Dai-ichi Shuppan Publishing Co. Ltd.; 2004 (in Japanese).
[18] Duggirala R, Villalpando CG, O'Leary DH, Stern MP, Blangero J. Genetic basis of variation in carotid artery wall thickness. Stroke 1996;27:833–7.
[19] Zannad F, Visvikis S, Gueguen R, et al. Genetics strongly determines the wall thickness of the left and right carotid arteries. Hum Genet 1998;103(2):183–8.
[20] O'Donnell CJ, Chazaro I, Wilson PWF, et al. Evidence for heritability of abdominal aortic calcific deposits in the Framingham Heart Study. Circulation 2002;106(3):337–41.
[21] Ilveskoski E, Perola M, Lehtimäki T, et al. Age-dependent association of apolipoprotein E genotype with coronary and aortic atherosclerosis in middle-aged men: an autopsy study. Circulation 1999;100(6):608–13.
[22] Pöllänen PJ, Lehtimäki T, Mikkelsson J, et al. Matrix metalloproteinase 3 and 9 gene promoter polymorphisms: joint action of two loci as a risk factor for coronary artery complicated plaques. Atherosclerosis 2005;180(1):73–8.
[23] Strong JP, Malcom GT, McMahan CA, et al. Prevalence and extent of atherosclerosis in adolescents and young adults: implications for prevention from the pathobiological determinants of atherosclerosis in youth study. JAMA 1999;281(8):727–35.
[24] Scheer WD, Boudreau DA, Hixson JE, et al. ACE insert/delete polymorphism and atherosclerosis. Atherosclerosis 2005;178(2):241–7.

ELSEVIER

Journal of the Neurological Sciences 243 (2006) 101 – 104

Journal of the Neurological Sciences

www.elsevier.com/locate/jns

Short communication

Pathology of the sympathetic nervous system corresponding to the decreased cardiac uptake in ^{123}I-metaiodobenzylguanidine (MIBG) scintigraphy in a patient with Parkinson disease

Jun Mitsui [a], Yuko Saito [b], Toshimitsu Momose [c], Jun Shimizu [a], Noritoshi Arai [a], Junji Shibahara [d], Yoshikazu Ugawa [a], Ichiro Kanazawa [a], Shoji Tsuji [a], Shigeo Murayama [b,*]

[a] *Department of Neurology, Division of Neuroscience, Graduate School of Medicine, the University of Tokyo, Tokyo, Japan*
[b] *Department of Neuropathology, Tokyo Metropolitan Institute of Gerontology, 35-2 Sakaecho, Itabashi-ku, Tokyo 173-0015, Japan*
[c] *Department of Nuclear Medicine, the University of Tokyo, Tokyo, Japan*
[d] *Department of Human Pathology, Graduate School of Medicine, the University of Tokyo, Tokyo, Japan.*

Received 25 January 2005; received in revised form 23 November 2005; accepted 23 November 2005
Available online 27 January 2006

Abstract

Decreased cardiac uptake in ^{123}I-metaiodobenzylguanidine (MIBG) scintigraphy has been adopted as one of the most reliable diagnostic tests for Parkinson disease (PD) in Japan. To investigate the morphological basis for this finding, we performed a detailed neuropathological study of the cardiac sympathetic nervous system of a 71-year-old autopsy-proven PD patient, who presented with a marked decrease in cardiac uptake of MIBG, just 1 year prior to death. We carefully examined the intermediolateral column at several levels of the thoracic spinal cord, the sympathetic trunk and ganglia, and the nerve plexus of the anterior wall of the left ventricle and compared the findings with those of five age-matched controls. We found that the cardiac plexus was more heavily involved than the sympathetic ganglia in this patient with PD. Our study may provide further evidence that the markedly decreased cardiac uptake of MIBG observed in PD cases represents preferential involvement of the cardiac sympathetic nerve plexus in this disorder.

Keywords: Lewy body; α-synuclein; Distal axonopathy

1. Introduction

^{123}I-metaiodobenzylguanidine (MIBG) is an analogue of noradrenaline and is metabolized by noradrenergic neurons. It is therefore used as a tracer in myocardial scintigraphy for the evaluation of cardiac sympathetic innervation. Markedly decreased cardiac uptake of MIBG shown by myocardial scintigraphy is a specific finding in Parkinson disease (PD) or dementia with Lewy bodies (DLB) and is useful for the differential diagnosis of other Parkinsonian syndromes [1–4] or Alzheimer's disease [5]. This decrement has been seen even in PD patients without autonomic symptoms [2–4].

A follow-up MIBG scintigraphy study recently revealed the occurrence of a progressive decrement of MIBG uptake in cases of Yahr Stage I PD (Dr. S. Orimo, abstract of the 45th Annual Meeting of the Japanese Association of Neurology, May 2004, Tokyo) while another report showed that PD patients with normal MIBG scintigraphy have a higher incidence of mutations of the *parkin* gene (Dr. M. Yamamoto, abstract of the 45th Annual Meeting of the Japanese Association of Neurology, May 2004, Tokyo). These observations suggest that the decreased uptake of MIBG is not necessarily a finding invariably observed in patients with levodopa-responsive-Parkinsonism.

Orimo et al. reported markedly decreased tyrosine hydroxylase (TH)-immunoreactive nerve fibers in the heart of a patient with pathologically proven PD, whose

* Corresponding author. Tel.: +81 3 3964 3241; fax: +81 3 3579 4776.
E-mail address: smurayam@tmig.or.jp (S. Murayama).

0022-510X/$ - see front matter © 2005 Elsevier B.V. All rights reserved.
doi:10.1016/j.jns.2005.11.034

cardiac uptake of MIBG had been found to be severely decreased 1 year before death [6]. Amino et al. reported that not only TH-immunoreactive but also neurofilament (NF)-immunoreactive nerve fibers were markedly decreased in heart tissues from patients with pathologically proven PD [7]. Recently, Orimo et al. examined heart tissues together with sympathetic ganglia from patients with pathologically proven PD, and concluded that although sympathetic ganglia were relatively preserved, TH-immunoreactive nerve fibers were markedly decreased in heart tissues [8].

Orimo's report is the only report describing an autopsy of a PD patient who had undergone MIBG scintigraphy in situ, because the examination is usually done in the very early clinical stage of the disorder. The purpose of this study was to examine in detail the neuropathological findings of the cardiac sympathetic nervous system in a patient with PD who was examined by MIBG scintigraphy 1 year prior to death.

2. Case report and methods

2.1. Case report

A 73-year-old right-handed man visited our outpatient clinic with chief complaints of progressive gait disturbance and bradykinesia. He had been well until 9 months before this visit, at which point he noticed slowness in walking and a tendency to fall backward. His gait disturbance and bradykinesia gradually deteriorated until he required help to rise from his bed. He had a past history of exposure to the atomic bomb in Hiroshima at age 19, at which time temporarily lost his hair. He also had an 11-year history of diabetes mellitus (DM) with excellent control using glibenclamide. On neurological examination, he showed mild rigidity in his neck and four extremities, severe bradykinesia and gait of short stride with loss of arm swing. His postural reflex was also impaired but resting tremor was absent. His deep tendon reflexes were preserved and no sensory disturbances were present and he did not have any symptoms of constipation, urinary disturbances or orthostatic hypotension.

The patient's fasting blood sugar was 106 mg/dl and his hemoglobin $A1_c$ was 6.0% (normal range: 4.3–5.8%). Magnetic resonance images of the brain were unremarkable except for mild cortical atrophy, and the electrocardiogram showed unremarkable results. The coefficient of variation of the R–R interval for the electrocardiogram was 1.03% (normal range: 1.27–3.69) but the head-up tilt test showed no evidence of orthostatic hypotension. Positron emission tomography (PET) studies showed reduced ^{18}F-fluorodopa uptake with mild laterality (right>left) and increased ^{11}C-*N*-methylspiperone uptake in the striatum with mild laterality (right<left), findings which were consistent with PD.

The patient received levodopa and experienced transient amelioration, but subsequently deteriorated into a wheelchair-bound state. At age 74, he had repeated hemorrhagic episodes from diverticulitis of the colon, subsequently followed by subacutely progressive dementia with a score by Mini-Mental Stage Examination of 3, one year and six months from the onset of Parkinsonism. He unexpectedly died of massive hemorrhage 5 months later. His clinical diagnosis was PD with dementia, following the "one year rule" of the Consensus Guidelines [9]. The total clinical course was 2 years.

2.2. MIBG myocardial scintigraphy

After the patient was in the supine position for 20 min, 111 MBq of ^{123}I-MIBG (Daiichi Radioisotope Laboratories Co, Tokyo, Japan) was intravenously injected. Planar imaging and single photon emission computed tomography were performed using a triple headed gamma camera (GCA9300A, Toshiba Co, Tokyo, Japan) after 15 min (early phase) and 3 h (late phase). Photopeak energy was centered at 159 keV with a 20% window and relative organ uptake of ^{123}I-MIBG was determined by setting the region of interest on the anterior planar image. Using average counts per pixel for the heart and mediastinum, the ratio of the uptake by the heart to that by the mediastinum was calculated.

2.3. Neuropathology

A postmortem examination was performed 18 h after death. The brain and spinal cord were fixed in 20% buffered formalin for two weeks and the appropriate areas were embedded in paraffin for routine morphological examinations. To study the cardiac sympathetic innervation in detail, the intermediolateral column at several levels of the thoracic spinal cord, the sympathetic trunk and ganglia, and the nerve plexus of the anterior wall of the left ventricle were carefully examined and compared with those of five age-matched controls.

Six micron-thick sections were stained with hematoxylin and eosin by the Klüver–Barrera method. Antibodies raised against Aβ (12B2, monoclonal, aa. 11–28, IBL, Maebashi, Japan); phosphorylated τ (ptau) (AT8, Innogenetics, Temse, Belgium); phosphorylated α-synuclein (psyn) (psyn#64, monoclonal, and Pser129, polyclonal, kind gifts from Dr T. Iwatsubo), phosphorylated neurofilament (SMI31, Sternberger Immunochemicals, Bethesda, MD); HLA-DR (CD68, Dako, Glostrup, Denmark); tyrosine hydroxylase (TH, polyclonal, Calbiochem, Parmstadt, Germany); and glial fibrillary acidic protein (GFAP, polyclonal, Dako, Glostrup, Denmark) were employed. The sections were visualized with a Ventana NX20 system as previously reported [10].

The control cases died of systemic disorders that did not affect the heart.

3. Results

3.1. MIBG myocardial scintigraphy

MIBG myocardial scintigraphy revealed that the uptake ratio of the heart to that of the mediastinum was 1.58 (normal mean of 2.76) during the early phase and 1.35 (normal mean of 3.45) during the late phase.

3.2. Neuropathology

The brain weighed 1250 g and the temporal lobe was slightly atrophic. Serial coronal slices of the brain showed mild dilatation of the lateral and third ventricles and serial axial sections revealed the loss of pigmentation in the substantia nigra and locus ceruleus. Histologically, neuronal loss and gliosis were present in the substantia nigra, locus ceruleus, and basal nucleus of Meynert. Lewy bodies (LBs) were present in the substantia nigra, locus ceruleus, dorsal vagal motor nucleus, raphe nucleus, hypothalamus, basal nucleus of Meynert, amygdala, anterior cingulate gyrus, transentorhinal region and second temporal gyrus, but not present in the frontal or parietal cortex. The LB score of this case was 4, following the Consensus Guidelines for DLB [9]. Senile plaques were absent and neurofibrillary tangles were only scattered in the transentorhinal cortex (Braak Stage I).

In the sympathetic nerves innervating the heart, LBs were present in the intermediolateral column of the thoracic spinal cord and sympathetic ganglia. In contrast, LBs were completely absent in the control subjects. Multiple levels of the intermediolateral column of the thoracic spinal cord were examined with anti-phosphorylated α-synuclein antibody (psyn). Scattered psyn-immunoreactive neuronal intracytoplasmic inclusions, threads and dots were present there. Immunohistochemistry with anti-psyn antibodies showed positive axons in the thoracic ventral roots, sympathetic trunk and cardiac plexus (Fig. 1D–F) and Nageotte's residual nodules were scattered among relatively preserved sympathetic ganglia (Fig. 1A). In the cardiac plexus, total loss of TH-immunoreactivity (Fig. 1H) compared with the normal control (Fig. 1G) and a marked decrease of axons (Fig. 1C) compared with the normal control (Fig. 1B) were evident. In contrast, the dorsal root ganglia and the sural nerve, including unmyelinated fibers, were well preserved, as shown by ultrastructural studies (data not shown). The heart itself did not show any valvular, coronary or myocardial change.

4. Discussion

This study found cardiac sympathetic denervation in a patient with PD, which was well correlated with severely decreased uptake in MIBG scintigraphy.

Previous studies demonstrated that neuronal degeneration with LBs occurs in broad areas of the sympathetic nervous system, including the sympathetic ganglia and the cardiac plexus, in patients with PD [11]. In the cardiac plexus, LBs and α-synuclein positive axons [12] or

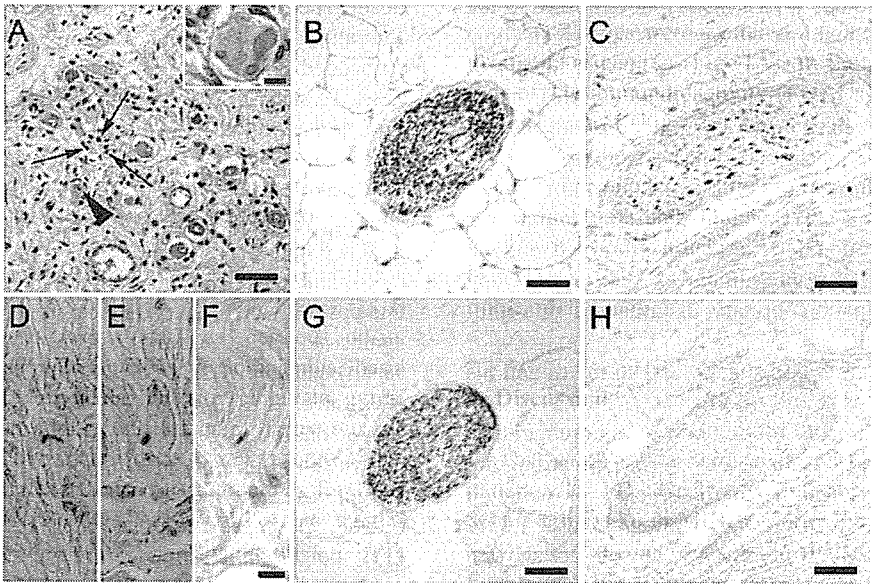

Fig. 1. Pathology of the sympathetic nervous system of a case of Parkinson disease A: a sympathetic ganglion showing a Nageotte's residual nodule (arrows) with Lewy bodies (LBs) (arrowhead) (hematoxylin and eosin staining, bar=50 μm). Inset: a typical LB in the sympathetic ganglion (bar=10 μm). B and C: unmyelinated fibers in the epicardial fatty tissue immunostained with anti-phosphorylated neurofilament antibody (SMI 31). Abundant axons from a control (B) and marked loss of axons from the case (C) (bar=50 μm). D–F: Lewy axons visualized by immunohistochemistry with anti-phosphorylated α-synuclein antibody (psyn#64) in the same fascicle as in section C (bar=10 μm). G and H: serial sections from section B (G) and C (H) immunoassayed with anti-tyrosine hydroxyls (TH) antibody. Abundant TH-immunoreactive fibers from the control (G) and total loss of immunoreactivity from the patient (H) (bar=50 μm).

markedly decreased TH-positive nerve fibers [7,8] were reported, which is consistent with our findings.

The present study found that the pathology of the sympathetic ganglia consisted of prominent α-synucleinopathy with a relatively preserved neuronal population. This was in sharp contrast with the severe axonal loss of sympathetic nerves in the cardiac muscle. Thus, LB-related α-synucleinopathy may cause distal axonopathy of the postganglionic sympathetic nerves.

It is difficult to exclude the possibility that the clinical history of DM may have made some contribution to the findings of MIBG scintigraphy and the pathology of the peripheral autonomic nervous system in this case, although the extremely low MIBG uptake and intact unmyelinated fibers in the sural nerve and dorsal root ganglia as well as pathologically unremarkable heart itself suggest that this possibility is not likely.

This study suggested that MIBG scintigraphy could be used to detect the presence of LB-related α-synucleinopathy in the cardiac sympathetic nervous system. Further prospective pathological studies on cardiac sympathetic innervation in PD or DLB patient who underwent MIBG scintigraphy should be carried out.

Acknowledgements

The authors thank Dr. Takeshi Iwatsubo (Department of Neuropathology and Neuroscience, Graduate School of Pharmaceutical Science, University of Tokyo) for kindly providing antibodies against phosphorylated α-synuclein and Ms. Azusa Uchinokura, Ms. Naoko Tokimura, Mr. Naoo Aikyo, Ms. Mieko Harada, and Ms. Nobuko Naoi for their technical support. This study was supported by Grants in Aid from the Tokyo Metropolitan Institute of Gerontology (S.M.) and from the Japanese Ministry of Education, Culture, Sports and Technology (Y.S.).

References

[1] Orimo S, Ozawa E, Nakade S, Sugimoto T, Mizusawa H. ^{123}I-metaiodobenzylguanidine myocardial scintigraphy in Parkinson's disease. J Neurol Neurosurg Psychiatry 1999;67:189–94.

[2] Taki J, Nakajima K, Kwang EH, Matsunari I, Komai K, Yoshita M, et al. Peripheral sympathetic dysfunction in patients with Parkinson's disease without autonomic failure is heart selective and disease specific. Eur J Nucl Med 2000;27:566–73.

[3] Braune S, Reinhardt M, Schnitzer R, Riedel A, Lücking CH. Cardiac uptake of [^{123}I] MIBG separates Parkinson's disease from multiple system atrophy. Neurology 1999;53:1020–5.

[4] Yoshita M. Differentiation of idiopathic Parkinson's disease from striatonigral degeneration and progressive supranuclear palsy using iodine-123meta-iodobenzylguanidine myocardial scintigraphy. J Neurol Sci 1998;155:60–7.

[5] Yoshita M, Taki J, Yamada M. A clinical role for [^{123}I] MIBG myocardial scintigraphy in the distinction between dementia of Alzheimer's-type and dementia with Lewy bodies. J Neurol Neurosurg Psychiatry 2001;71:583–8.

[6] Orimo S, Ozawa E, Oka T, Nakade S, Tsuchiya K, Yoshimoto M, et al. Different histopathology accounting for a decrease in myocardial MIBG uptake in PD and MSA. Neurology 2001;57:1140–1.

[7] Amino T, Orimo S, Itoh Y, Takahashi A, Uchichara T, Mizusawa H. Profound cardiac sympathetic denervation occurs in Parkinson disease. Brain Pathol 2005;15:29–34.

[8] Orimo S, Amino T, Itoh Y, Takahashi A, Kojo T, Uchichara T, et al. Cardiac sympathetic denervation precedes neuronal loss in the sympathetic ganglia in Lewy body disease. Acta Neuropathol 2005; 109:583–8.

[9] McKeith I.G., Galasko D, Kosaka K, Perry EK, Dickson DW, Hansen LA, et al. Consensus guidelines for the clinical and pathologic diagnosis of dementia with Lewy bodies (DLB): report of the consortium on DLB international workshop. Neurology 1996;47: 1113–24.

[10] Saito Y, Kawashima A, Ruberu NN, Fujiwara H, Koyama S, Sawabe M, et al. Accumulation of phosphorylated α-synuclein in aging human brain. J Neuropathol Exp Neurol 2003;62:644–54.

[11] Wakabayashi K, Takahashi H. Neuropathology of autonomic nervous system in Parkinson's disease. Eur Neurol 1997;38(Suppl 2):2–7.

[12] Iwanaga K, Wakabayashi K, Yoshimoto M, Tomita I, Satoh H, Takashima H, et al. Lewy body-type degeneration in cardiac plexus in Parkinson's and incidental Lewy body diseases. Neurology 1999;52: 1269–71.

Neuropathology and Applied Neurobiology (2006), **32**, 374–387 doi: 10.1111/j.1365-2990.2006.00736.x

Comparison of extent of tau pathology in patients with frontotemporal dementia with Parkinsonism linked to chromosome 17 (FTDP-17), frontotemporal lobar degeneration with Pick bodies and early onset Alzheimer's disease

A.-M. Shiarli[1], R. Jennings[1], J. Shi[1,2], K. Bailey[1], Y. Davidson[1], J. Tian[1,2], E. H. Bigio[3], B. Ghetti[4], J. R. Murrell[4], M. B. Delisle[5], S. Mirra[6], B. Crain[7], P. Zolo[8], K. Arima[9], E. Iseki[10], S. Murayama[11], H. Kretzschmar[12], M. Neumann[12], C. Lippa[13], G. Halliday[14], J. MacKenzie[15], N. Khan[16], R. Ravid[17], D. Dickson[18], Z. Wszolek[18], T. Iwatsubo[19], S. M. Pickering-Brown[1,18] and D. M. A. Mann[1]

[1]*Clinical Neuroscience Research Group, University of Manchester, Greater Manchester Neurosciences Centre, Hope Hospital, Salford, UK,* [2]*Department of Care of the Elderly, Dongzhimen Hospital, Beijing University of Chinese Medicine, Beijing, China,* [3]*North western University Alzheimer's Disease Center, Chicago, IL, USA,* [4]*Indiana Alzheimer Disease Centre, Indiana University School of Medicine, Indianapolis, IN, USA,* [5]*Service d'Anatomie et de Cytologie Pathologiques, Hopitaux de Toulouse, Toulouse, Cedex 4, France,* [6]*Department of Pathology, State University of New York Health Science Center at Brooklyn, Brooklyn, NY, USA,* [7]*Department of Pathology, Johns Hopkins University School of Medicine, Baltimore, MD, USA,* [8]*San Donato Medical Center, Arezzo, Italy,* [9]*National Centre Hospital for Mental, Nervous and Muscular Disorders, Tokyo, Japan,* [10]*Juntendo Tokyo Koto Geriatric Medical Center, Juntendo University School of Medicine, Tokyo, Japan,* [11]*Department of Neuropathology, Tokyo Metropolitan Institute of Gerontology, Tokyo, Japan,* [12]*Reference Centre for Prion Diseases and Neurodegenerative Diseases, Institute of Neuropathology, Marchioninistr 17, Munchen, Germany,* [13]*Memory Disorders Centre, Drexel University College of Medicine, Philadelphia, PA, USA,* [14]*Department of Neuropathology, Prince of Wales Medical Research Institute, University of New South Wales, Randwick, NSW, Australia,* [15]*The Royal Infirmary, Foresterhill, Aberdeen, Scotland,* [16]*The Brain Bank, Institute of Psychiatry, London, UK,* [17]*Netherlands Brain Bank, Meibergdreef 33, Amsterdam, the Netherlands,* [18]*Mayo Clinic, 4500 San Pablo Road, Jacksonville, FL, USA,* [19]*Department of Neuropathology and Neuroscience, University of Tokyo, Tokyo, Japan*

A.-M. Shiarli, R. Jennings, J. Shi, K. Bailey, Y. Davidson, J. Tian, E. H. Bigio, B. Ghetti, J. R. Murrell, M. B. Delisle, S. Mirra, B. Crain, P. Zolo, K. Arima, E. Iseki, S. Murayama, H. Kretzschmar, M. Neumann, C. Lippa, G. Halliday, J. MacKenzie, N. Khan, R. Ravid, D. Dickson, Z. Wszolek, T. Iwatsubo, S. M. Pickering-Brown and D. M. A. Mann (2006) *Neuropathology and Applied Neurobiology* 32, 374–387

Comparison of extent of tau pathology in patients with frontotemporal dementia with Parkinsonism linked to chromosome 17 (FTDP-17), frontotemporal lobar degeneration with Pick bodies and early onset Alzheimer's disease

In order to gain insight into the pathogenesis of frontotemporal lobar degeneration (FTLD), the mean tau load in frontal cortex was compared in 34 patients with frontotemporal dementia linked to chromosome 17 (FTDP-17) with 12 different mutations in the *tau* gene (*MAPT*), 11 patients with sporadic FTLD with Pick bodies and 25 patients with early onset Alzheimer's disease (EOAD). Tau load was determined, as percentage of tissue occupied by stained product, by image analysis of immunohistochemically stained sections using the phospho-dependent antibodies AT8, AT100 and AT180. With AT8 and AT180 antibodies, the amount of tau was significantly ($P < 0.001$

Correspondence: David M. A. Mann, Clinical Neuroscience Research Group, University of Manchester, Greater Manchester Neurosciences Centre, Hope Hospital, Salford, M6 8HD, UK. Tel: +44 0161 206 2580; Fax: +44 0161 206 0388; E-mail: david.mann@manchester.ac.uk

in each instance) less than that in EOAD for both FTDP-17 (8.5% and 10.0% respectively) and sporadic FTLD with Pick bodies (16.1% and 10.0% respectively). With AT100, the amount of tau detected in FTDP-17 was 54% ($P < 0.001$) of that detected in EOAD, but no tau was detected in sporadic FTLD with Pick bodies using this particular antibody. The amount of insoluble tau deposited within the brain in FTDP-17 did not depend in any systematic way upon where the *MAPT* mutation was topographically located within the gene, or on the physiological or structural change generated by the mutation, regardless of which anti-tau antibody was used. Not only does the amount of tau deposited in the brain differ between the three disorders, but the pattern of phosphorylation of tau also varies according to disease. These findings raise important questions relating to the role of aggregated tau in neurodegeneration – whether this represents an adaptive response which promotes the survival of neurones, or whether it is a detrimental change that directly, or indirectly, brings about the demize of the affected cell.

Keywords: Tau protein, Tau gene, Alzheimer's disease, frontotemporal lobar degeneration, neurofibrillary tangle, Pick bodies

Introduction

Frontotemporal lobar degeneration (FTLD) is a descriptive term given to a clinically and pathologically heterogeneous group of early onset, non-Alzheimer forms of dementia. A previous family history of a similar disorder occurs in about half of patients, and a consensus conference in 1997 highlighted the observations that many such families were linked to a locus on chromosome 17, following which the term frontotemporal dementia with Parkinsonism linked to chromosome 17 (FTDP-17) was derived [1]. In 1998, the disorder was shown [2–4], in certain of these chromosome 17-linked families, to be associated with mutational events in the *tau* gene (*MAPT*), located on the long arm of chromosome 17 (17q21–22). The prevalence of *MAPT* mutations within patients with FTLD varies from about 6–18% [5–7].

To date, more than 35 *MAPT* mutations in over 150 families have been identified, and there is much clinical as well as pathological heterogeneity among the various mutations (see [8,9] for reviews). Some *MAPT* mutations exist as missense mutations within coding regions of exons 1, 9, 11, 12 and 13 [2,3,6,10–19]. Generally, cases with these mutations show swollen nerve cells, and rounded intraneuronal inclusions, reminiscent of the Pick bodies typically seen in some cases of sporadic FTLD, mainly within large and small pyramidal neurones of the cerebral cortex and pyramidal and granule cells of the hippocampus [10–19]. These mutations affect all six isoforms of tau and generate mutated tau molecules that (variably) lose their ability to interact with microtubules, thereby interfering with the promotion of microtubule assembly and axonal transport [2,3,6,10–20]. Some of the mutations also increase, but again variably, the propensity of the mutated tau to self-aggregate into fibrils that form the characterizing pathological structures within the brain [14–16,18–20].

Other *MAPT* mutations lie close to the splice donor site of the intron that follows the alternatively spliced exon 10 [2–4,6,20–35]. Such cases typically show insoluble aggregated tau deposits as neurofibrillary tangle (NFT)-like structures within large and smaller pyramidal cells of cortical layers III and V, and prominently within glial cells in the deep white matter, globus pallidus and internal capsule [23,27,30–34,36,37]. This group of mutations cluster around, or lie within a predicted regulatory stem loop structure of a splice acceptor domain of *MAPT* that determines the inclusion or exclusion of exon 10 by alternative splicing during gene transcription. Such mutations may destabilize this stem loop, and disrupt its function, interfering with the binding of U1snRNP splice regulatory elements, increasing the proportion of tau mRNA transcripts containing exon 10, and the amount of 4-repeat (4R) tau, relative to 3-repeat (3R) tau, protein [2,3]. Other mutations within exon 10 interfere with the splicing ratio between 3R and 4R tau either by strengthening [22,26,35] or destroying [26] the function of splicing-enhancing elements, or by disrupting the function of a splice-silencing element [26,31], in the 5′ region of exon 10. Exon 10 mutations like P301L do not affect the splicing of exon 10 [2,26] but induce conformational changes in tau molecules containing exon 10 that interfere with microtubule function, and lead to a specific aggregation of the mutant 4R tau into fibrils [31,35].

Surveys of the published literature infer that not only the distribution and morphology of the insoluble tau aggregate vary greatly in patients with FTLD with *MAPT* mutations according to mutation site and type, but also the total amount of deposited tau can differ. Microscopic observation of cases of FTDP-17 with those of younger individuals with early onset Alzheimer's disease (EOAD) suggests a lower burden of tau pathology. Such observations are somewhat curious and paradoxical given the prevailing view that *MAPT* mutations are the root cause of clinical disability in FTDP-17, whereas in Alzheimer's disease (AD) tau pathology is considered to be a more downstream (to amyloid pathology) event. They also challenge the hypothesis that the accumulation of tau within nerve cells is detrimental to the health of the cell and responsible for its demize.

In the present study we have therefore measured, by image analysis of tau-immunostained sections, and compared the amount of insoluble tau proteins (tau load) in the brains of patients with FTDP-17 with 12 different *MAPT* mutations, patients with sporadic FTLD with Pick bodies and other patients with EOAD.

Materials and methods

Brain tissues were available at autopsy from 34 cases of FTDP-17 with 12 different *MAPT* mutations. Six cases (cases #19–24), one with *MAPT* exon 10 +13 mutation (case #19), and five with *MAPT* exon 10 +16 mutation (cases #20–24) were obtained from the Manchester Brain Bank [37], whereas tissue samples from the other 28 FTDP-17 cases were kindly supplied in collaboration by colleagues from different centres across the world. Selected clinical and pathological details for all cases are given in Table 1. Full clinical and pathological descriptions for 31 of the 34 cases of FTDP-17 have been previously reported by the originating authors (see Table 1 for details of citation); the other three cases remain unreported to date. The 34 FTDP-17 cases (18 men and 16 women) (see Table 1) had mean age of onset of disease of 48.5 ± 7.8 years, range 32–65 years with mean age of death was 57.3 ± 10.0 years, range 38–78 years. The mean disease duration was 8.5 ± 5.5 years, range 2–27. Twelve cases had *APOE* ε3/ε3 genotype, seven had ε3/ε4 genotype, five had ε2/ε3 genotype and one was ε2/ε2. Only in cases #19 and 20 were there any additional AD-type changes, and then only in the form of some diffuse amyloid plaques. Neither case had sufficient AD-type pathology to warrant (additional) diagnosis of AD under Consortium to Establish a Registry for Alzheimer's Disease (CERAD) criteria [38]. Braak staging (for AD) [39] was inappropriate.

Tissues were also obtained from 11 cases of sporadic FTLD (cases #35–45) from the Manchester Brain Bank collection, in whom previous pathological investigations [37 and unpublished Mann *et al.*] had shown Pick bodies to be present in the cerebral cortex and hippocampus. Pick bodies were identified, as defined by Kertesz *et al.* [40], as round or oval, compact intracytoplasmic neuronal inclusions, stained by Bielschowsky but not by Gallyas, tau-immunoreactive and located in dentate fascia, hippocampus and cerebral cortex. The 11 cases (six men and five women) had a mean age of onset of disease of 57.6 ± 10.4 years, range 46–76 years and mean age of death 66.5 ± 9.2 years, range 56–84 years. The mean disease duration was 8.9 ± 2.7 years, range 4–14 years. Five patients had *APOE* ε3/ε3 genotype, two had ε3/ε4 genotype, two had ε2/ε3 genotype and one was ε2/ε2. None of these cases showed any coincidental AD-type pathology.

All 25 cases of EOAD (11 men and 14 women) were from the Manchester Brain Bank collection. These had a mean age of onset of disease of 53.4 ± 6.6 years, range 35–60 years and mean age of death 62.9 ± 8.0 years, range 44–73 years. The mean disease duration was 9.5 ± 3.5 years, range 4–19 years. Sixteen patients had *APOE* ε3/ε3 genotype, seven had ε3/ε4 genotype, one had ε2/ε3 genotype and one had ε2/ε2 genotype. All cases were consistent with CERAD pathological criteria for AD [38], and all were at Braak stages 5 or 6 [39]. In none of the cases was there a previous family history of disease consistent with autosomal dominant inheritance.

We chose not to include a control group of nondemented persons within the study because the primary purpose was to investigate how the level of tau deposition in FTLD compared with that in EOAD. Moreover, the great majority of cases studied, FTLD or AD, were less than 65 years of age at death, and it is uncommon for significant tau pathology to be present in normal individuals in that age range. Furthermore, although cases of corticobasal degeneration (CBD) and progressive supranuclear palsy (PSP) are subsumed under some pathological criteria for FTLD [41], we did not include such cases in this present study. This was because in CBD, tau pathology is within glial cells as well as neurones, and principally affects parietal cortex rather than frontal lobes, whereas

Table 1. Selected clinical and pathological details of cases investigated

Case	*Diagnosis*	MAPT *mutation*	*Gender*	*Age at onset (year)*	*Age at death (year)*	*Duration (year)*	APOE *genotype*	*Brain weight (g)*
1 [18]	FTDP-17	L266V	M	32	36	3.5	NA	1050
2 [30]	FTDP-17	N279K	M	46	57	11	3,3	1250
3 [30]	FTDP-17	N279K	M	44	50	6	3,3	1420
4 [20]	FTDP-17	N279K	M	44	50	6	3,4	1290
5 [20]	FTDP-17	N279K	F	45	48	3	3,3	1100
6 [20]	FTDP-17	N279K	M	56	58	2	2,3	1400
7 [20]	FTDP-17	N279K	F	45	53	8	2,4	1000
8 [20]	FTDP-17	N279K	M	57	63	6	3,4	1100
9 [20]	FTDP-17	N279K	M	41	52	11	2,3	1100
10 [25]	FTDP-17	N279K	M	40	47	7	NA	1230
11 [33]	FTDP-17	N296H	M	57	62	3	3,3	960
12 [6,21]	FTDP-17	P301L	M	48	60	12	3,3	1331
13 [6,21]	FTDP-17	P301L	F	50	66	15	3,3	856
14 [6,21]	FTDP-17	P301L	M	44	52	8	2,3	1087
15 [6,21]	FTDP-17	P301L	F	54	76	22	2,2	1006
16 [6,21]	FTDP-17	P301L	F	59	64	5	3,3	1013
17 [28]	FTDP-17	P301L	F	48	55	7	NA	915
18 [32,36]	FTDP-17	S305S	F	48	51	3	NA	1053
19 [2,34]	FTDP-17	Exon 10 +13	M	65	70	5	3,4	1100
20 [2,34]	FTDP-17	Exon 10 +16	M	50	61	11	3,4	1016
21 [2,34]	FTDP-17	Exon 10 +16	F	46	58	12	3,3	996
22 [2,34]	FTDP-17	Exon 10 +16	M	43	55	12	3,4	1240
23 [34]	FTDP-17	Exon 10 +16	F	52	65	13	2,3	1040
24 [34]	FTDP-17	Exon 10 +16	F	48	56	8	3,4	1175
25 [un]	FTDP-17	Exon 10 +16	F	43	52	9	2,3	1138
26 [19]	FTDP-17	Q336R	M	58	68	10	3,3	1102
27 [12]	FTDP-17	G342V	F	48	55	7	3,3	1020
28 [15]	FTDP-17	K369I	F	52	61	9	NA	885
29 [13]	FTDP-17	G389R	F	32	37	5	3,3	1006
30 [un]	FTDP-17	G389R	M	45	49	4	NA	1170
31 [11]	FTDP-17	G389R	M	38	43	5	NA	NA
32 [6,21]	FTDP-17	R406W	M	63	70	7	3,3	1121
33 {6,21]	FTDP-17	R406W	F	58	71	13	3,4	905
34 [un]	FTDP-17	R406W	F	49	78	29	NA	1035
35 [37]	Pick	None	F	53	60	7	3,3	960
36 [37]	Pick	None	M	46	56	10	3,3	1150
37 [37]	Pick	None	M	NA	NA	NA	NA	NA
38 [37]	Pick	None	F	52	62	10	3,4	928
39 [37]	Pick	None	F	76	84	8	3,3	1235
40 [37]	Pick	None	F	50	58	8	2,2	1065
41 [37]	Pick	None	M	63	74	11	2,3	990
42 [37]	Pick	None	M	73	77	4	3,3	NA
43 [37]	Pick	None	F	57	64	7	3,3	1000
44 [37]	Pick	None	M	47	61	14	3,4	980
45 [un]	Pick	None	M	59	69	10	2.3	NA
46	AD	None	F	54	59	5	3,3	1008
47	AD	None	F	56	62	6	3,3	1020
48	AD	None	M	55	60	5	3,4	1368
49	AD	None	F	57	67	10	3,4	1018
50	AD	None	F	39	45	6	3,3	NA
51	AD	None	M	40	44	4	3,3	1400
52	AD	None	F	52	71	19	3,3	910
53	AD	None	M	35	45	10	3,4	1177

Table 1. *Continued*

Case	*Diagnosis*	MAPT *mutation*	*Gender*	*Age at onset (year)*	*Age at death (year)*	*Duration (year)*	APOE *genotype*	*Brain weight (g)*
55	AD	None	F	58	70	12	3,4	1026
56	AD	None	F	52	61	9	3,3	906
57	AD	None	F	52	64	12	2,2	1120
58	AD	None	F	54	67	13	3,3	947
59	AD	None	M	55	61	6	3,3	NA
60	AD	None	M	60	72	12	3,4	1251
61	AD	None	F	60	73	13	3,3	1028
62	AD	None	F	52	61	9	3,3	1262
63	AD	None	M	56	66	10	3,3	1070
64	AD	None	F	59	71	12	3,3	1208
65	AD	None	M	55	64	9	2,3	1275
66	AD	None	F	48	60	12	3,4	1050
67	AD	None	M	59	64	5	3,3	1330
68	AD	None	M	57	67	10	3,3	1158
69	AD	None	M	60	66	6	3,3	1206
70	AD	None	M	58	70	12	3,4	1314

FTDP-17, frontotemporal dementia with Parkinsonism linked to chromosome 17; Pick, frontotemporal lobar degeneration with Pick bodies; AD, Alzheimer's disease; un, unpublished case. NA, no details available. Citation numbers in parentheses.

in PSP, tau pathology is mostly within neurones and glial cells in subcortical structures. Therefore, although such disorders can likewise be considered as tauopathies, measurement of tau load within frontal cortex was not considered to be informative, at least as regards the purpose of the present investigation.

Serial sections from formalin-fixed, wax-embedded blocks of frontal cortex (BA 8/9) were cut at a thickness of 6 μm and mounted on 3-aminopropyltrieihoxysilane (APES)-coated slides. Sections were immunostained for insoluble tau proteins by a standard immunoperoxidase method [37], using the phospho-dependent tau antibodies AT8 (1 : 750 dilution), AT100 (1 : 200 dilution) and AT180 (1 : 200 dilution) (all from Innogenetics, Belgium). AT8 antibody is raised against phosphorylated Ser202 epitope and immunoreacts with paired helical filament (PHF) tau in AD [42]. AT100 antibody is raised against phosphorylated Thr212/Ser214 epitopes and labels only pathological tau [43]. AT180 antibody is raised against phosphorylated Thr231 epitope, and labels approximately 70% of PHF in AD brain, but also labels phosphorylated foetal and adult normal tau [44].

The amount of insoluble tau (tau load) within AT8-, AT100- and AT180-immunostained sections was quantified by Image Analysis. The system employed uses Leica Image Analysis software and a Leica Microscope with Quantimet 570 Image Analyser. Measurement of tau load was performed only on grey matter regions. The area for measurement, which extended from the surface of the cortex to the grey/white matter boundary, was identified under the microscope at ×5 magnification. After optimizing the computer captured image for colour and staining density, the total measured area and area of tissue occupied by stained product were determined using in-house software. The software employed allows the segmented image to be directly overlaid upon the captured image so that with optimal thresholding it can be ensured that all tau-immunostained stained objects (for example, NFT, neuropil threads and plaque neurites in AD, NFT or Pick bodies in FTLD and FTDP-17) are recognized. To ensure comparability between cases, the particular area measured was systematically sampled so that the measured field was always on a 'straight' section of the cortex, away from the depths or the crown of the gyrus, and away from 'bad quality tissue' (that is, tissue areas containing artefactual staining or splits or tears in the section). The total area of cortex measured in each field averaged 1.43 mm^2. Tau load was calculated as the percentage of total area occupied by immunostained product. Trial measurements, employing cumulative mean statistic, were initially performed to determine the number of fields required to be measured for the mean to fall within 95% confidence levels for each antibody. In this way it was determined that for AT8-immunostained sections six measurements were

necessary, and for AT100- and AT180-immunostained sections four measurements were required. The mean tau load was calculated for each section.

Image Analysis data was analysed using the Statsdirect statistical package. Because the mean tau load data obtained from AT8-immunostained sections did not follow a normal distribution, logarithmic transformation was performed. A one way analysis of variance test (ANOVA) was then used to compare differences in tau deposition between each disease group with *post hoc* unpaired *t*-tests being performed where results of ANOVA were significant. The tau load data obtained for sections stained with AT100 and AT180 likewise did not follow a normal distribution, even when logarithmically transformed. Therefore, Kruskal–Wallis test was used to compare differences in tau deposition between each disease group with *post hoc* Mann–Whitney *U*-tests being performed when result of Kruskal–Wallis was significant. Comparison of tau load between bearers and non-bearers of *APOE* ε4 allele in each disease group were performed for all antibodies using Mann–Whitney *U*-test. For all statistical tests a *P*-value less than 0.05 was considered significant.

In order to investigate the effect of different *MAPT* mutations on tau load, the cases were categorized into four groups according to mutation type:

Group A – cases ($n = 18$) with *MAPT* mutations which affect splicing of exon 10 increasing the 4R : 3R ratio of tau isoforms and producing mostly NFT pathology (mutations: N279K, N296H, S305S, +16, +13).

Group B – cases ($n = 16$) with *MAPT* mutations which alter the tau protein and have been shown to affect microtubule binding (mutations: L266V, Q336R, G342V, K369I, G389R, P301L, R406W).

Group C – cases ($n = 7$) with *MAPT* mutations which alter the tau protein and have been shown to affect microtubule binding, but produce only Pick-type pathology (mutations: L266V, Q336R, G342V, K369I, G389R).

Group D – cases ($n = 9$) with *MAPT* mutations which alter the microtubule binding of the protein, but do not affect exon 10 splicing, and produce mostly NFT-type pathology (mutations: P301L, R406W)

Mann–Whitney *U*-tests were performed between these groups to investigate differences in tau deposition between different groups of *MAPT* mutations. Mann–Whitney *U*-test was also performed to investigate differences in tau deposition between FTDP-17 group C cases with Pick-type bodies and sporadic FTLD cases with Pick bodies. Mann–Whitney *U*-tests were also performed to assess differences in relative immunoreactivity between AT8, AT100 and AT180 antibodies, for each disease group. Spearman rank correlation test was used to determine correlations between tau load and duration and age of onset of disease in each disease group.

Results

Morphological descriptions of tau pathology, using the present, or other similar, tau antibodies, on those FTDP-17 patients studied here have been fully reported previously by both ourselves [13,19,34,37] and other workers [6,10–12,15,18,25,28,30,32–34,36], as have those patients with sporadic FTLD with Pick bodies from our own series of FTLD cases [37], and such observations are therefore not repeated in this present study. Likewise, the immunohistochemical pattern of tau pathology in the AD cases was entirely typical of the disorder, and is likewise not described further in this report.

Comparison of tau load between the three disease groups

Mean tau load detected for each disease group, for each antibody, is shown in Table 2. For AT8 antibody, there was a highly significant difference in tau load between the three disease groups ($F_{2,67} = 44.4$; $P < 0.0001$) so that mean tau load in FTDP-17, and in sporadic FTLD with Pick bodies, were both significantly less ($P < 0.001$) than that in EOAD. There was a trend ($P = 0.057$) towards

Table 2. Mean (± SD) tau load in frontal cortex as detected by phospho-dependent antibodies AT8, AT100 and AT180 in 34 patients with FTDP-17, 11 with sporadic FTLD with Pick bodies and 25 with EOAD

	AT8	*AT100*	*AT180*
FTDP-17	1.2 ± 1.1	1.5 ± 1.5	0.9 ± 0.8
MAPT mutation Group A	1.1 ± 1.2	1.1 ± 1.5	0.7 ± 0.9
MAPT mutation Group B	1.4 ± 1.0	2.0 ± 1.4	1.0 ± 0.6
MAPT mutation Group C	1.7 ± 1.2	1.6 ± 1.5	0.8 ± 0.5
MAPT mutation Group D	1.1 ± 0.8	2.2 ± 1.3	1.2 ± 0.7
Sporadic FTLD with Pick bodies	2.3 ± 1.5	0 ± 0	0.9 ± 0.6
EOAD	14.3 ± 12.8	2.8 ± 3.1	9.0 ± 11.0

FTDP-17, frontotemporal dementia with Parkinsonism linked to chromosome 17; FTLD, frontotemporal lobar degeneration; EOAD, early onset Alzheimer's disease.

mean tau load in FTDP-17 being less than that in sporadic FTLD with Pick bodies.

For AT180 antibody, using Kruskal–Wallis test, there was a highly significant difference in mean tau load between the three disease groups ($\chi^2 = 27.9$; $P < 0.0001$) so that mean tau load in FTDP-17, and in sporadic FTLD with Pick bodies, was significantly less ($P < 0.001$) than that in EOAD. There was no significant difference ($P = 0.918$) in mean tau load between FTDP-17 and sporadic FTLD with Pick bodies.

For AT100 antibody (again using Kruskal–Wallis test) there was also a highly significant difference in mean tau load between the three disease groups ($\chi^2 = 24.5$; $P < 0.0001$). Indeed, there was little or no (measurable) staining of Pick bodies with AT100. Mean tau load in FTDP-17, and in EOAD, was consequently greater ($P < 0.001$) than that in sporadic FTLD with Pick bodies. Mean tau load in FTDP-17 was less (but not significantly so, $P = 0.083$) than that in patients with EOAD.

Differences in tau deposition within the FTDP-17 group

The extent of tau deposition was compared in FTDP-17 according to *MAPT* mutation position or type. When plotted against the topographical position of the *MAPT* mutation (coding for the longest tau isoform), no clear cut individual differential effect of any of the *MAPT* mutations on the extent of tau deposition within the frontal cortex was seen, either for AT8, AT100 or AT180 antibodies (Figure 1). Nonetheless, with AT8 immunostaining, *MAPT* L266V and exon 10 +13 splice mutation showed

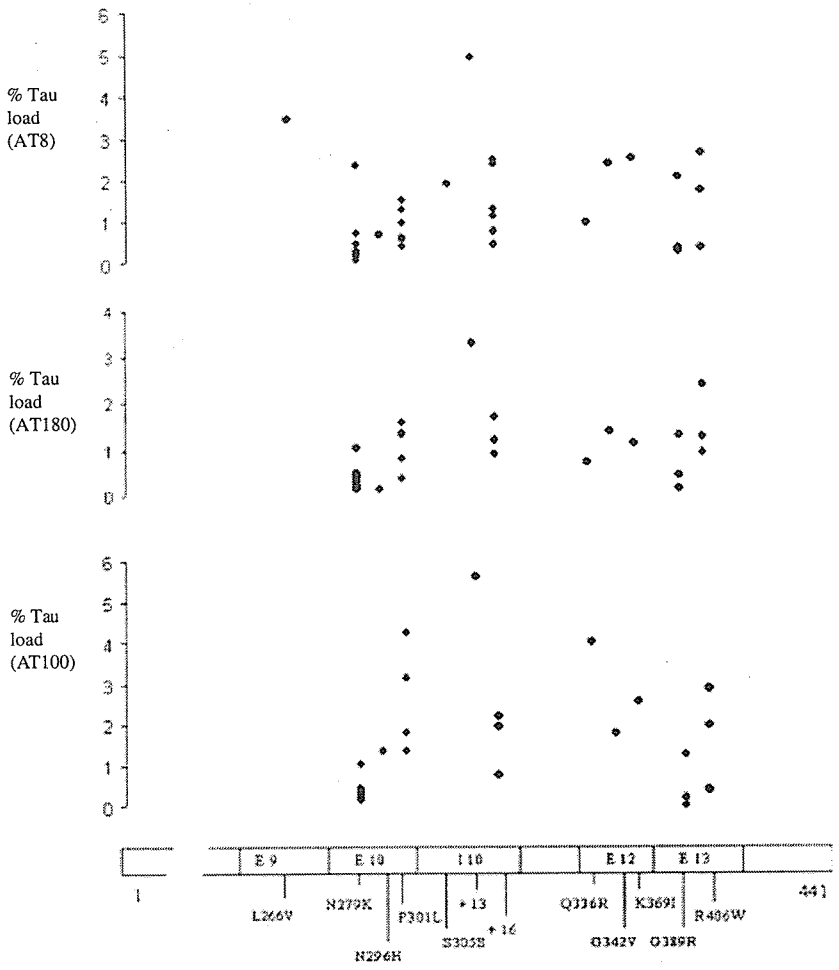

Figure 1. Tau load detected in each case for each of the mutations; E indicates exons on the gene; I indicates intron.

particularly heavy tau deposition, relative to the other cases. For L266V, this is consistent with the involvement of all the cortical layers of grey matter and some astrocytic staining in the pathological process (see also [18]). In the exon 10 +13 mutation, this could be explained by the presence of many tau-positive neuritic plaques in the superficial layers of the cortex (see also [34]). For AT180, again as explained, exon 10 +13 splice mutation showed particularly heavy tau deposition. However, for AT100 some of P301L cases, and the Q336R case, were heavily stained relative to AT8 and AT100 (Figure 1).

As detailed in *Methods* section, the mutation cases were grouped in order to investigate the effect of different *MAPT* mutation types on tau load. No significant differences in mean tau load were seen between any of the four *MAPT* mutation groups as detected by either AT8 ($\chi^2 = 1.05$; $P = 0.789$), AT180 ($\chi^2 = 2.86$; $P = 0.413$) or AT100 ($\chi^2 = 6.52$; $P = 0.09$) antibodies (Table 2). The mean tau load in FTDP-17 cases with Pick-type bodies (that is, Group C cases) did not differ from that seen in sporadic FTLD with Pick bodies for either AT8 ($P = 0.375$) or AT180 antibodies ($P = 0.887$) (Table 2), although interestingly AT100 immunostained Pick bodies in Group C cases (cf lack of Pick body staining in sporadic FTLD with Pick bodies).

Comparisons of relative immunoreactivities of each antibody

In general, in FTDP-17, AT8 and AT100 gave similar degree of immunostaining, whereas AT180 antibody showed less immunoreactivity (Table 2), although for some *MAPT* mutations (for example, R406W, N279K, exon 10 +16, G389R mutations) the tau load detected by AT8 and AT180 antibodies was similar. Again, in general, AT100 antibody showed slightly more immunoreactivity than AT8, but in some instances AT8 and AT100 immunoreactivity was the same (for example, K369I, G342V, exon 10 +13 mutations) and for some (for example, P301L mutation) AT100 gave stronger staining than AT8. However, statistically, the mean tau load detected by AT8, AT100 or AT180 antibodies did not vary significantly ($\chi^2 = 2.1$; $P = 0.340$) (Table 2).

In sporadic FTLD with Pick bodies, and EOAD, mean tau load detected by each antibody varied significantly ($\chi^2 = 24.8$ and $\chi^2 = 22.4$ respectively; $P < 0.0001$ for both). *Post hoc* testing showed that in both of these disease groups, mean tau load detected by AT8 was greater than that detected by either AT100 ($P < 0.0001$ in both instances) or AT180 ($P = 0.004$ and $P = 0.026$ respectively), and that mean tau load detected by AT180 was greater than that detected by AT100 in both disease groups ($P < 0.0001$ in both instances).

Effect of possession of the *APOE* ε4 allele

Mean percentage tau load, as detected by AT8, AT100 or AT180 antibodies, in patients with *APOE* ε4 allele was not significantly different from that detected in those without *APOE* ε4 allele for any of the three disorders (Table 3)

Correlations with age of onset of disease and duration of illness

With AT8, no significant correlation between duration of illness and tau load was found for any of the three disorders ($r_s = 0.07$–0.09; $P = 0.595$–0.838). For the age of onset of disease no significant correlations were found

Table 3. Mean (±SD) tau load in frontal cortex as detected by phospho-dependent antibodies AT8, AT100 and AT180 in 34 patients with FTDP-17, 11 with sporadic FTLD with Pick bodies and 25 with EOAD, stratified into those bearing *APOE* ε4 allele and those without *APOE* ε4 allele

	APOE status	*AT8*	*AT100*	*AT180*
FTDP-17	With ε4 allele	1.7 ± 1.7	1.5 ± 1.6	1.2 ± 1.3
	Without ε4 allele	0.9 ± 0.7	1.9 ± 2.1	0.8 ± 0.6
Sporadic FTLD with Pick bodies	With ε4 allele	2.3 ± 1.5	0 ± 0	0.7 ± 0.8
	Without ε4 allele	2.3 ± 0.3	0 ± 0	1.0 ± 0.7
EOAD	With ε4 allele	15.0 ± 12.5	2.9 ± 3.3	12.5 ± 13.0
	Without ε4 allele	13.5 ± 12.5	2.8 ± 3.2	7.6 ± 10.3

FTDP-17, frontotemporal dementia with Parkinsonism linked to chromosome 17; FTLD, frontotemporal lobar degeneration; EOAD, early onset Alzheimer's disease.

with tau load for either FTDP-17 ($r_s = 0.09$; $P = 0.623$) or EOAD ($r_s = 0.37$; $P = 0.070$), but a significant inverse correlation was found in sporadic FTLD with Pick bodies ($r_s = -0.850$; $P = 0.002$). Similar findings were seen with AT100 and AT180 (data not shown).

Discussion

The effect of 12 different mutations in *MAPT* on the amount of tau protein deposited in the brain has been investigated in this study using immunohistochemical staining with three phosphorylation-dependent anti-tau antibodies. We grouped the mutations according to their functional effects, or pathological characteristics, looking for differences in effect between those mutations (Group A) which affect splicing of exon 10 increasing the 4R : 3R ratio of tau isoforms and produce mostly NFT pathology with those missense mutations outside exon 10 (Group B) that change the protein structure of tau and affect all tau isoforms and interfere with microtubule binding. We also compared mutations that generate a Pick body-like pathology (Group C) with those that alter the microtubule-binding capability of tau, but do not affect exon 10 splicing and produce mostly NFT-type pathology (Group D). In no instance did we find any significant group differences in the extent of tau deposition with any of the antibodies, nor did any single mutation appear to have any preferential effect in this respect, although singleton cases of L266V and exon 10 +13 splice mutation did show relative (to other mutations) high tau loads with AT8 and AT180. In the former case there were unusually high levels of tau within grey matter astrocytes [see, also 18], while in the latter case there was a heavy tau burden within neuritic plaques [see 34], in accordance with age and possession of *APOE* ε4 allele [45]. Some P301L cases and the single Q336R case showed disproportionately (relative to AT8 and AT180) high tau loads with AT100. Hence, we find that the amount of tau deposited in the brain in FTDP-17 does not seem to be determined either by topographic position within *MAPT*, or the physiological change in tau function induced by such a mutation. Neither does the isoform composition of the aggregated tau seem to influence the amount of tau deposited because there was no difference in tau load between Group B cases, which lead to a tau deposition with a mix of (mostly) 3R and 4R tau isoforms [see 10–13,15,18,19], and Group A cases, where the tau protein is known to be mostly, or only, 4R [see 22,25,28,30–34,36]. This implies that both types of mutation, despite having a different primary effect on the tau protein itself, ultimately affect cellular function (possibly microtubule stability) in a similar way and/or to a similar degree. Similarly, the amount of tau deposited in the form of Pick bodies in FTDP-17 is not different from that seen in cases of sporadic FTLD characterized by Pick body formation.

Interestingly, and perhaps paradoxically, the amount of tau deposited in FTDP-17 or in FTLD with Pick bodies, irrespective of the physiological change in tau invoked (that is, mutational or posttranslational respectively), as detected by AT8 and AT180 antibodies, was about one-tenth of that deposited in EOAD. Because the cases were matched for age at onset and duration of disease, it is unlikely that these differences in tau load reflect demographic variations or differences in stage of the disease at death. Indeed, there were no correlations between tau load and duration of illness for any of the disease groups. However, because, in AD at least [46,47], tau proteins are incorporated into aggregated filamentous structures on a whole molecule basis, and not as a series of (variably) truncated molecules, it might be argued that variations in tau load between disorders using these two antibodies reflect differences in degree of phosphorylation of tau at different epitopes, or ease of antibody accessibility, rather than actual number of tau molecules present. These considerations are unlikely to explain the very high differences in tau load between FTLD and EOAD with AT8 antibody at least, because biochemical measures of insoluble tau load by Western blot using this particular antibody have also shown much greater quantities of insoluble tau within the brain in AD compared with FTLD cases (Hasegawa, unpub. data). Present data suggest therefore that there is a lower accumulation of pathological tau over the span of the illness in the brains of patients with FTLD, irrespective of underlying cause, compared with those with AD. The reason for this lower tissue accumulation of tau lies mostly with differing anatomical compartmentalization. In AD the pathological tau deposits are present within neuronal cell bodies (as NFT), dendrites (as neuropil threads) and in axon terminals in neuritic plaques. Tau load in AD, as measured here, represents the composite total of these three anatomical compartments. However, in FTDP-17, and in FTLD with Pick bodies, the bulk of the pathological tau is perikaryal, with little neuropil staining in most instances, except as above where there may be additional glial tau or neuritic plaques present.

The results obtained with AT100 antibody are interesting. AT100 labels pathological aggregations of the PHF in NFT in AD, but does not label normal tau [43]. This antibody detects phosphorylated epitopes Thr212/Ser214 in PHF with the epitope being achieved by the sequential phosphorylation of tau at Thr212 by GSK-3β, then at Ser214 by protein kinase A (PKA) in the presence of polyanions such as heparin and tRNA [48]. In this present study, there was little or no immunoreactivity with AT100 in cases of FTLD with Pick bodies, in contrast to cases of AD and FTDP-17. This suggests that in FTLD with Pick bodies either the requirements needed for the formation of the AT100 epitope [48] are not fulfilled, and the epitope is therefore not phosphorylated, or that the tertiary structure of tau in Pick bodies upon fixation makes the epitope inaccessible even though it may be phosphorylated. Maillot and co-workers [49] have detected, by Western blot, insoluble tau in brain tissue of cases of FTLD with Pick bodies using AT100, implying that this epitope is indeed phosphorylated, and that changes in the conformational structure of Pick bodies on tissue fixation may be masking the AT100 epitope. This is quite possible, because low or no Pick body immunoreactivity has been observed with another phosphorylation-dependent antibody, 12E8, raised against the Ser262 epitope [37,50]. However, in this instance, it was also not possible, using 12E8, to detect tau proteins from FTLD cases with Pick bodies on Western blotting [49], implying that a non-phosphorylation of this particular epitope is responsible for the lack of detection of tau in Pick bodies. In AD [51] and *MAPT* exon 10 +16 [34,37] cases, 12E8 specifically stains well-formed NFT rather than pretangles; AT100, likewise, stains NFT strongly, and pretangles less strongly [43]. Nonetheless, in another study, Ferrer and colleagues used a different (to 12E8) antibody against Ser262 epitope (Ser^{262}), which in AD stains pretangles, and showed Pick bodies to be strongly reactive [52]. Hence, the reason for the lack of Pick body staining with AT100 is still not clear.

Also of particular note are findings in *MAPT* P301L mutation where AT100 antibody stained tau aggregations much more strongly than the other two antibodies, in contrast to other *MAPT* mutations where AT8 was usually strongest (see Figure 1). It is therefore possible that protein conformational changes induced by this mutation may help to fulfil the requirements for formation of the Thr212/Ser214 epitope [48]. However, the Ser202 (AT8) epitope needs to be phosphorylated before formation of the AT100 epitope [48], yet in P301L mutation AT8 immunoreactivity was less than that of AT100. This suggests that conformational changes of tau protein, potentially induced by P301L mutation, confer a lesser accessibility of the AT8 antibody to its epitope, which although phosphorylated is relatively undetected, while in contrast such changes enhance the detection of the AT100 Thr212/Ser214 epitope.

On face value, present findings might therefore suggest that FTLD is a pathologically 'less aggressive' illness than AD. Because there is greater tissue loss in FTLD than in AD, it might be argued that the accumulation of aggregated tau proteins within neurones in FTLD is incidental and epiphenomenal to the main disease process that leads to the gross neurodegeneration seen in these cases. However, it may also be the case that *MAPT* mutations cause changes in cellular function so lethal to the nerve cell that death occurs before (many of) the cells can accumulate (much) tau. One direct effect of the *MAPT* missense mutations leads to formation of mutated tau molecules that lose ability to bind microtubules and reduce microtubule assembly resulting in impaired axonal transport [22]. Exon 10 mutations increase the ratio between 4R : 3R tau and perturb the precisely regulated stoichiometric binding of tau proteins to tubulin needed for microtubule assembly [53]. Hence, catastrophic disruption in protein transport leading to cell death may occur in many neurones without significant tau accumulation having taken place.

It has been shown that unpolymerized hyperphosphorylated tau proteins in the cell cytosol can sequester normal functional tau, forming filaments and leading to inhibition and disassembly of microtubules [54]. However, polymerized tau in the form of PHF does not possess this ability [55]. In AD, neurones may therefore 'promote' PHF formation from hyperphosphorylated tau in order to protect normal cytosolic tau from being sequestered into filaments, thereby allowing cells to survive longer [56]. Because tau in AD is neither mutated nor produced in a stoichiometrically unbalanced way, it is possible therefore that microtubule formation and function can be maintained (longer than in FTLD) despite the accumulation of PHF. Tau aggregation may therefore be a protective or an adaptive response of neurones. Due to the catastrophic effect of *MAPT* mutations on microtubule function, this process in FTLD is inefficient or ineffective, and many nerve cells die without ever accumulating (much) tau. Only those (relatively few) nerve cells better able to resist